Study of J/ψ Production in Jets

R. Aaij *et al.*[*]
(LHCb Collaboration)

(Received 19 January 2017; published 8 May 2017)

The production of J/ψ mesons in jets is studied in the forward region of proton-proton collisions using data collected with the LHCb detector at a center-of-mass energy of 13 TeV. The fraction of the jet transverse momentum carried by the J/ψ meson, $z(J/\psi) \equiv p_{\rm T}(J/\psi)/p_{\rm T}(\text{jet})$, is measured using jets with $p_{\rm T}(\text{jet}) > 20$ GeV in the pseudorapidity range $2.5 < \eta(\text{jet}) < 4.0$. The observed $z(J/\psi)$ distribution for J/ψ mesons produced in b-hadron decays is consistent with expectations. However, the results for prompt J/ψ production do not agree with predictions based on fixed-order nonrelativistic QCD. This is the first measurement of the $p_{\rm T}$ fraction carried by prompt J/ψ mesons in jets at any experiment.

DOI: 10.1103/PhysRevLett.118.192001

The production of J/ψ mesons in hadron-hadron collisions occurs at the transition between the perturbative and nonperturbative regimes of quantum chromodynamics (QCD), resulting in a rich phenomenology that is yet to be fully understood. Differential J/ψ production cross sections measured at both the Tevatron [1,2] and the LHC [3–9] can be described using the nonrelativistic QCD (NRQCD) [10–12] effective field theory approach. However, many NRQCD-based calculations [13–15] predict a large degree of transverse polarization, whereas minimal polarization is observed in data [16–19]. This discrepancy indicates that further studies are needed to gain a better understanding of J/ψ production.

Quarkonium production is often used as a probe of QCD phenomenology [20]. In proton-lead (pPb) collisions, J/ψ production is used to study cold-nuclear-matter effects such as parton shadowing and nuclear absorption [21–23], while hadron melting in the quark-gluon plasma is investigated using J/ψ production in PbPb collisions [24–26]. Double-J/ψ production is used to measure the effective cross section for double parton scattering [27–31], which is commonly assumed to be universal for all processes. If the prevailing picture of J/ψ meson production directly in parton-parton scattering is not valid, then many quarkonium-production results may need to be reinterpreted.

Another striking, yet untested, prediction of the direct-production paradigm is that J/ψ mesons are largely produced isolated, except for any soft gluonic radiation emitted by the $c\bar{c}$ state and potentially some particles from the underlying hadron-hadron collision. An alternative to the standard approach, which is also based on NRQCD, is the calculation of J/ψ meson production within jets using either analytic resummation [32] or the parton shower of a Monte Carlo event generator [33]. Quarkonium production in the parton shower, which can explain the lack of observed polarization [34], predicts that J/ψ mesons are rarely produced in isolation. Consequently, it is of great interest to study the radiation produced in association with quarkonium states, e.g., J/ψ mesons in jets, to distinguish between these two different pictures of quarkonium production.

This Letter reports a study of J/ψ mesons produced in jets in the forward region of pp collisions. The fraction of the jet transverse momentum carried by the J/ψ meson, $z(J/\psi) \equiv p_{\rm T}(J/\psi)/p_{\rm T}(\text{jet})$, is measured for J/ψ mesons produced promptly and for those produced in b-hadron decays. The data sample corresponds to an integrated luminosity of 1.4 fb^{-1} collected at a center-of-mass energy of $\sqrt{s} = 13$ TeV with the LHCb detector in 2016. Only events containing exactly one reconstructed pp collision are used as these provide the best resolution on $p_{\rm T}(\text{jet})$. The analysis is performed using jets clustered with the anti-$k_{\rm T}$ algorithm [35] using a distance parameter $R = 0.5$ and within the following kinematic fiducial region: jets are required to have $p_{\rm T}(\text{jet}) > 20$ GeV ($c = 1$ throughout this Letter) in the pseudorapidity range $2.5 < \eta(\text{jet}) < 4.0$; J/ψ mesons, which are reconstructed using the $J/\psi \to \mu^+\mu^-$ decay, must satisfy $2.0 < \eta(J/\psi) < 4.5$; and muons are required to have $p_{\rm T}(\mu) > 0.5$ GeV, $p(\mu) > 5$ GeV, and $2.0 < \eta(\mu) < 4.5$. No requirements are placed on the multiplicity of jets per event or particles per jet, so that jets consisting of only a J/ψ candidate are allowed. This is the first measurement of $z(J/\psi)$ in prompt J/ψ production at any experiment.

The LHCb detector is a single-arm forward spectrometer covering the range $2 < \eta < 5$, described in detail in Refs. [36,37]. Simulated data samples are used to evaluate the muon reconstruction efficiency, the detector response for jet reconstruction, and to validate the analysis. In the

[*]Full author list given at the end of the article.

simulation, pp collisions are generated using PYTHIA8 [38] with a specific LHCb configuration [39]. Decays of hadronic particles are described by EVTGEN [40], in which final-state radiation is generated using PHOTOS [41]. The interaction of the generated particles with the detector, and its response, are implemented using the GEANT4 toolkit [42] as described in Ref. [43].

The online event selection is performed by a trigger [44], which consists of a hardware stage using information from the calorimeter and muon systems, followed by a software stage, which performs the J/ψ candidate reconstruction. The hardware stage selects events with at least one dimuon candidate with $\sqrt{p_{\mathrm{T}}(\mu^+)p_{\mathrm{T}}(\mu^-)}$ greater than a threshold that varied between 1.3 and 1.5 GeV during the 2016 data taking. In the software stage, two muon candidates with $p_{\mathrm{T}}(\mu) > 0.5$ GeV are required to form a J/ψ candidate whose invariant mass is within 150 MeV of the known J/ψ mass [45]. Additional selection criteria are applied offline to the J/ψ candidates: the tracks are required to satisfy stringent muon-identification criteria; and the muon and J/ψ candidates are required to be within the fiducial region of this analysis, where the detector is well understood.

A new data-taking scheme was introduced by LHCb in 2015 that enables offline-like performance in the online system. The alignment and calibration are performed in near real time [46] and are available in the trigger reconstruction [47]. Furthermore, an increase in the online CPU resources makes it possible to run the offline track reconstruction in the online system. This analysis is based on a data sample where all online-reconstructed particles in the event are stored, but most lower-level information is discarded, greatly reducing the event size. This data-storage strategy makes it possible to record all events containing a J/ψ candidate without placing any requirements on $p_{\mathrm{T}}(J/\psi)$, or on the displacement of the J/ψ decay from the primary vertex (PV).

Jet reconstruction is performed offline on this data sample by clustering the J/ψ candidates with charged and neutral particle-flow candidates [48], all reconstructed online, using the anti-k_{T} clustering algorithm as implemented in FASTJET [49]. This is the first LHCb analysis to use online-reconstructed particles that were not involved in the trigger decision. The J/ψ candidates, rather than their component muons, are used in the clustering to prevent muons from a single J/ψ decay being clustered into separate jets. Reconstructed jets with $p_{\mathrm{T}}(\mathrm{jet}) > 15$ GeV and $2.5 < \eta(\mathrm{jet}) < 4.0$ are kept for further analysis, where jets in the $p_{\mathrm{T}}(\mathrm{jet})$ range 15–20 GeV are retained for use in unfolding the detector response. The $\eta(\mathrm{jet})$ requirement, which is included in the fiducial region definition, ensures a nearly uniform resolution of 20%–25% on the p_{T} of the non-J/ψ component of the jet, with minimal p_{T} dependence above 10 GeV. This is similar to the resolution achieved on data events [48] when using offline reconstruction for p_{T} below 20 GeV, but worse at higher p_{T} where the resolution in such events is about 15%. This degradation arises largely because calorimeter information not associated with particle-flow candidates is not stored in this data sample.

The jet momenta are not corrected for reconstruction bias. Instead, the effect of the detector response on the $z(J/\psi)$ distributions is removed using an unfolding procedure. This involves first determining the reconstructed J/ψ yields in bins of $[z(J/\psi), p_{\mathrm{T}}(\mathrm{jet})]$, then correcting them for detection efficiency. Bin migration, which occurs largely due to the resolution on the non-J/ψ component of the jet, is accounted for by unfolding the $[z(J/\psi), p_{\mathrm{T}}(\mathrm{jet})]$ distributions of corrected J/ψ yields using an iterative Bayesian procedure 50,51]] (see the Supplemental Material [52] for a detailed discussion of the unfolding). Finally, the unfolded $[z(J/\psi), p_{\mathrm{T}}(\mathrm{jet})]$ distributions are integrated for $p_{\mathrm{T}}(\mathrm{jet}) > 20$ GeV to produce the measured $z(J/\psi)$ spectra. The binning scheme employs ten equal-width $z(J/\psi)$ bins, and three $p_{\mathrm{T}}(\mathrm{jet})$ bins of 15–20, 20–30, and > 30 GeV.

The yield of $J/\psi \to \mu^+\mu^-$ decays reconstructed in each $[z(J/\psi), p_{\mathrm{T}}(\mathrm{jet})]$ bin, which includes J/ψ mesons produced promptly and in b-hadron decays, is determined from an unbinned maximum likelihood fit to the corresponding dimuon invariant-mass distribution. The signal component is modeled as the sum of two Crystal Ball functions [53] that share all shape parameters except the width. The combinatorial background is described by an exponential function. Both the signal and background shapes are allowed to vary in each bin independently. An example of the invariant-mass distribution from one $[z(J/\psi), p_{\mathrm{T}}(\mathrm{jet})]$ bin is shown in Fig. 1 along with the fit result. The total J/ψ signal yield in the data sample is almost 2×10^6.

The fraction of J/ψ mesons that originates from b-hadron decays is determined by fitting the distribution of the pseudodecay-time $\tilde{t} \equiv \lambda m(J/\psi)/p_{\mathrm{L}}(J/\psi)$, where λ denotes the difference in position along the beam axis between the J/ψ decay and primary vertices, $m(J/\psi)$ is the known J/ψ

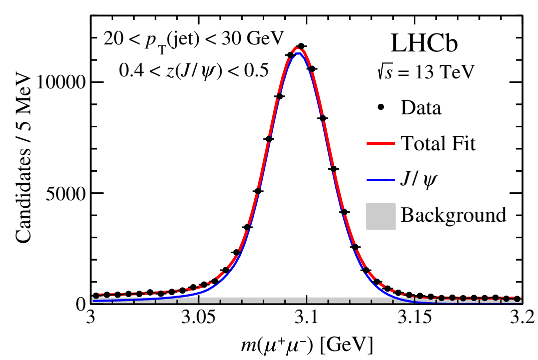

FIG. 1. Example dimuon invariant-mass distribution with the fit result superimposed from the bin $[0.4 < z(J/\psi) < 0.5, 20 < p_{\mathrm{T}}(\mathrm{jet}) < 30$ GeV$]$. The signal is modeled as the sum of two Crystal Ball functions, while the background is described by an exponential function.

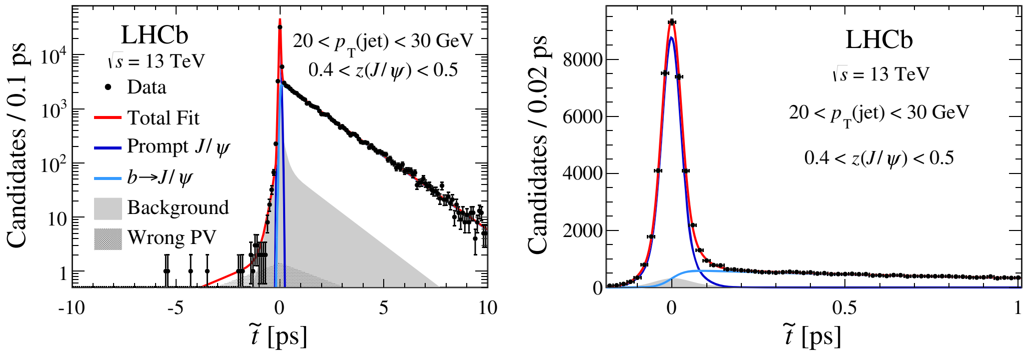

FIG. 2. Example pseudo-decay-time distribution from the same bin as in Fig. 1 with the fit result superimposed. The right plot shows the $[-0.2, 1]$ ps region on a linear scale.

mass [45], and $p_L(J/\psi)$ is the component of the J/ψ momentum longitudinal to the beam axis. Only candidates with $|\tilde{t}| < 10$ ps, corresponding to about seven b-hadron lifetimes, and a mass consistent with the known J/ψ mass are used in these unbinned maximum likelihood fits. The $\tilde{t}$ distribution from one $[z(J/\psi), p_T(\text{jet})]$ bin is shown in Fig. 2. The prompt-J/ψ component is modeled by a Dirac δ function, while the b-hadron component is modeled by an exponential decay function with a variable lifetime parameter; both are convolved with a double-Gaussian resolution function. A long and nearly symmetric tail in the $\tilde{t}$ distribution arises due to J/ψ candidates produced in additional pp collisions that are not reconstructed. The shape of this component, the contribution of which is found to be $\mathcal{O}(0.1\%)$ in all bins, is modeled by constructing the distribution with $\tilde{t}$ calculated using J/ψ and PV candidates from different data events. Finally, the shape of the non-J/ψ component in each bin is parametrized using an empirical function obtained from a fit to the $\tilde{t}$ distribution observed in the $m(\mu^+\mu^-)$ sidebands, while its normalization is fixed from the $m(\mu^+\mu^-)$ fit in the bin. The fraction of J/ψ mesons that are produced in b-hadron decays is determined to be in the range 20%–60%, depending on the $[z(J/\psi), p_T(\text{jet})]$ bin.

The J/ψ yields are corrected for detection efficiency by applying per-candidate weights of $\epsilon_{\text{tot}}^{-1}$, where ϵ_{tot} is the total detection efficiency determined as the product of the reconstruction, selection, and trigger efficiencies. The use of per-candidate weights within a fiducial region where the efficiency is nonzero throughout produces accurate efficiency-corrected yields without requiring knowledge of the $J/\psi \to \mu^+\mu^-$ angular distribution or, equivalently, the J/ψ polarization. The weights, which are similar for nearly all candidates, are rarely greater than 5 and never greater than 20. Consequently, there is negligible impact on the statistical variance due to the use of weighted candidates, since the vast majority of events in each $[z(J/\psi), p_T(\text{jet})]$ bin contribute nearly equally.

The muon reconstruction efficiency is obtained from simulation in bins of $[p(\mu), \eta(\mu)]$. Scale factors that correct for discrepancies between the data and simulation are determined using a data-driven tag-and-probe approach on an independent sample of $J/\psi \to \mu^+\mu^-$ decays [54]. A small $p_T(J/\psi)$-dependent correction is applied to the yields of J/ψ mesons produced in b-hadron decays to account for a drop in the efficiency at large b-hadron flight distances. Within the fiducial region of this analysis, the J/ψ reconstruction efficiency is on average about 90%.

The dominant contribution to the selection inefficiency is from the muon-identification performance, which is measured in bins of $[p_T(\mu), \eta(\mu)]$ using a highly pure calibration data sample of $J/\psi \to \mu^+\mu^-$ decays. The efficiency of selecting a reconstructed J/ψ candidate varies from 80% for $z(J/\psi) \lesssim 0.1$ to nearly 100% for $z(J/\psi) \gtrsim 0.5$. The trigger efficiency is measured in bins of $[\sqrt{p_T(\mu^+)p_T(\mu^-)}, \eta(J/\psi)]$ using a subset of this J/ψ calibration sample. Events selected by the hardware trigger independently of the J/ψ candidate, e.g., due to the presence of a high-p_T hadron, are used to determine the trigger efficiency directly from the data. The fraction of J/ψ candidates in each $[\sqrt{p_T(\mu^+)p_T(\mu^-)}, \eta(J/\psi)]$ bin that are selected by the dimuon hardware trigger gives the efficiency, which is about 40% on average for $z(J/\psi) \lesssim 0.1$ and 80% for $z(J/\psi) \gtrsim 0.5$.

The effects of $[z(J/\psi), p_T(\text{jet})]$ bin migration, which are predominantly due to the detector response to the non-J/ψ component of the jet, are corrected for using an unfolding technique [50–52]. The detector-response matrices for J/ψ mesons produced promptly and in b-hadron decays are dissimilar for two reasons: the p_T -dependent particle multiplicities are different, and the undetected momentum carried by K^0 and Λ particles is, on average, larger for jets that contain a b-hadron decay. The $p_T(\text{jet})$ -dependent mean and width of the reconstructed particle multiplicity distributions for jets in simulation are adjusted to match those observed in data. The detector response is studied using the p_T -balance distribution of $p_T(\text{jet})/p_T(Z)$ in nearly back-to-back Z + jet events using the same data-driven technique as in Ref. [48]. Small adjustments are applied to the $p_T(\text{jet})$ scale and resolution in simulation obtaining the best agreement with data. The unfolding

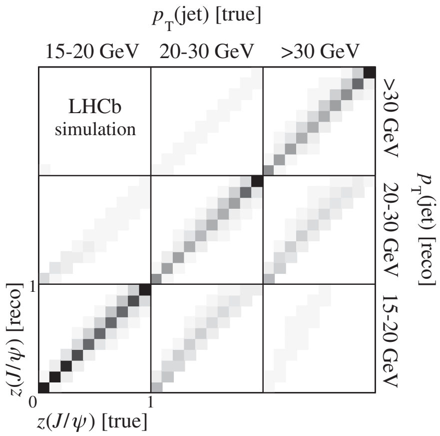

FIG. 3. The four-dimensional detector-response matrix for prompt J/ψ production. The shading represents the bin-to-bin migration probabilities ranging from (white) 0 to (black) 1, with the lightest shade of gray corresponding to a probability of 0.1%–0.3%. Jets whose true p_T(jet) is above 20 GeV but whose reconstructed p_T(jet) is below 15 GeV, or *vice versa*, are included in the unfolding but not shown graphically.

matrix for jets that contain a prompt J/ψ meson is shown in Fig. 3, while the corresponding matrix for b-hadron production is provided in the Supplemental Material [52].

Systematic uncertainties on the $z(J/\psi)$ distributions apply to both the prompt and b-hadron production modes. Uncertainty on the J/ψ yields arises from the efficiency corrections and from possible mismodeling of the components in the invariant-mass and pseudo-decay-time fits. The uncertainty on each component of the total efficiency is assessed by repeating the data-driven efficiency studies on simulated events, where the difference between the true and efficiency-corrected J/ψ yields in bins of $[p_T(J/\psi), \eta(J/\psi)]$ is used to determine the systematic uncertainty. The relative uncertainty on the reconstruction efficiency is determined to be 2%, which includes the unknown J/ψ polarization. The relative uncertainties on the trigger and selection efficiencies are in the ranges 2%–5% and 0%–2%, respectively, depending on the $[z(J/\psi), p_T(\text{jet})]$ bin.

The uncertainty on the total J/ψ yield obtained from the invariant-mass fits (1%) is studied by replacing the nominal signal and background models with single Crystal Ball and quadratic functions, respectively. The relative uncertainty on the fraction of J/ψ mesons produced in b-hadron decays (1%) is determined by comparing the fit results obtained from simulated $\tilde{t}$ distributions to the true fractions. Potential mismodeling of the non-J/ψ and wrong-PV components is found to contribute negligible uncertainty. The total relative uncertainty on the J/ψ yields is 3%–6% depending on the $[z(J/\psi), p_T(\text{jet})]$ bin, which corresponds to a bin-dependent absolute uncertainty on $z(J/\psi)$ of 0.001–0.005.

The uncertainty associated with the detector response to the non-J/ψ component of the jet is studied by building alternative unfolding matrices, where the p_T scale and resolution are varied within the uncertainties obtained from the data-driven p_T -balance study of $Z+$jet events. The data are unfolded using these alternative matrices, with the differences in the $z(J/\psi)$ distribution used to assign $z(J/\psi)$ -dependent absolute uncertainties of 0.001–0.014. The p_T(jet) and $z(J/\psi)$ spectra used to generate the unfolding matrices, along with the unfolding procedure itself, are also potential sources of uncertainty. These are studied by simulating data samples similar to the experimental data, then unfolding them using response matrices constructed from p_T(jet) and $z(J/\psi)$ distributions that are different from those used to generate the samples. Based on these studies, an uncertainty of 0.01 is assigned to each $z(J/\psi)$ bin due to unfolding. Finally, the uncertainties due to the fragmentation model and due to the K^0 and Λ components of the jet are found to be negligible. The total absolute systematic uncertainty in each $z(J/\psi)$ bin, which dominates over the statistical one, is 0.010–0.015.

The measured normalized $z(J/\psi)$ distributions for J/ψ mesons produced promptly and for those produced in b-hadron decays are shown in Fig. 4 (the numerical values are provided in Ref. [52]). The b-hadron results are consistent with the PYTHIA8 prediction [52], where the uncertainty shown is due to b-quark fragmentation [55,56] (other sources of uncertainty are ignored [52]). The prompt-J/ψ results do

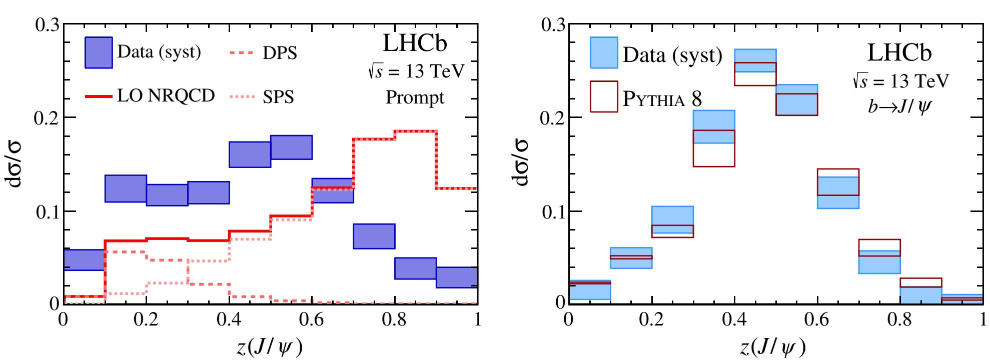

FIG. 4. Measured normalized $z(J/\psi)$ distributions for J/ψ mesons produced (left) promptly and (right) in b-hadron decays, compared to predictions obtained from PYTHIA8. The statistical uncertainties are negligible. The (DPS) double and (SPS) single parton scattering contributions to the prompt prediction are also shown (the DPS effective cross section in PYTHIA8 is 31 mb).

not agree with the leading-order (LO) NRQCD-based prediction as implemented in PYTHIA8, which includes both color-octet and color-singlet mechanisms using long-distance matrix elements determined empirically [52]. At small $z(J/\psi)$, PYTHIA8 predicts that most $p_{\mathrm{T}}(\mathrm{jet})$ arises from a parton-parton scatter other than the one that produced the J/ψ meson. The dominant source of uncertainty on the prompt-J/ψ prediction at large $z(J/\psi)$ is due to the underlying event; however, since no rigorous method exists for determining this uncertainty, no uncertainty is assigned to the prediction. Given that the underlying event at LHCb is well described by PYTHIA8, e.g., the energy flow is accurately predicted at the 5% level [57], the prompt-J/ψ results cannot be reconciled with this prediction. Furthermore, LO and partial next-to-leading-order (NLO*) calculations in both the color-singlet and color-octet models similarly fail to describe the data [52,58].

Prompt J/ψ mesons in data are observed to be much less isolated than predicted, which qualitatively agrees with the alternative picture of quarkonium production presented in Ref. [32] (after this Letter was submitted, Ref. [59] demonstrated quantitative agreement). The lack of isolation observed for prompt J/ψ production may be related to the long-standing quarkonium polarization puzzle. If high-p_{T} J/ψ mesons are predominantly produced within parton showers, rather than directly in parton-parton scattering, then the observed lack of both polarization and isolation could be explained [34]. Future related measurements of J/ψ production in jets should help shed light on the nature of quarkonium production [60,61].

In summary, the production of J/ψ mesons in jets is studied using pp-collision data collected by LHCb at $\sqrt{s} = 13$ TeV in the fiducial region: $p_{\mathrm{T}}(\mathrm{jet}) > 20$ GeV and $2.5 < \eta(\mathrm{jet}) < 4.0$; $2.0 < \eta(J/\psi) < 4.5$; and $p_{\mathrm{T}}(\mu) > 0.5$ GeV, $p(\mu) > 5$ GeV, and $2.0 < \eta(\mu) < 4.5$. The fraction of the jet p_{T} carried by the J/ψ meson is measured for J/ψ mesons produced promptly and for those produced in b-hadron decays. The observed distribution for J/ψ mesons produced in b-hadron decays is consistent with the PYTHIA8 prediction; however, the prompt-J/ψ results do not agree with predictions based on fixed-order NRQCD as implemented in PYTHIA8.

We express our gratitude to our colleagues in the CERN accelerator departments for the excellent performance of the LHC. We thank the technical and administrative staff at the LHCb institutes. We acknowledge support from CERN and from the national agencies: CAPES, CNPq, FAPERJ and FINEP (Brazil); NSFC (China); CNRS/IN2P3 (France); BMBF, DFG and MPG (Germany); INFN (Italy); FOM and NWO (The Netherlands); MNiSW and NCN (Poland); MEN/IFA (Romania); MinES and FASO (Russia); MinECo (Spain); SNSF and SER (Switzerland); NASU (Ukraine); STFC (United Kingdom); NSF (USA). We acknowledge the computing resources that are provided by CERN, IN2P3 (France), KIT and DESY (Germany), INFN (Italy), SURF (The Netherlands), PIC (Spain), GridPP (United Kingdom), RRCKI and Yandex LLC (Russia), CSCS (Switzerland), IFIN-HH (Romania), CBPF (Brazil), PL-GRID (Poland) and OSC (USA). We are indebted to the communities behind the multiple open source software packages on which we depend. Individual groups or members have received support from AvH Foundation (Germany), EPLANET, Marie Skłodowska-Curie Actions and ERC (European Union), Conseil Général de Haute-Savoie, Labex ENIGMASS and OCEVU, Région Auvergne (France), RFBR and Yandex LLC (Russia), GVA, XuntaGal and GENCAT (Spain), Herchel Smith Fund, The Royal Society, Royal Commission for the Exhibition of 1851 and the Leverhulme Trust (United Kingdom).

[1] D. Acosta *et al.* (CDF Collaboration), Measurement of the J/ψ meson and b-hadron production cross sections in $p\bar{p}$ collisions at $\sqrt{s} = 1960$ GeV, Phys. Rev. D **71**, 032001 (2005).

[2] S. Abachi *et al.* (D0 Collaboration), J/ψ production in $p\bar{p}$ collisions at $\sqrt{s} = 1.8$ TeV, Phys. Lett. B **370**, 239 (1996).

[3] R. Aaij *et al.* (LHCb Collaboration), Measurement of forward J/ψ production cross-sections in pp collisions at $\sqrt{s} = 13$ TeV, J. High Energy Phys. 10 (2015) 172.

[4] R. Aaij *et al.* (LHCb Collaboration), Production of J/ψ and Υ mesons in pp collisions at $\sqrt{s} = 8$ TeV, J. High Energy Phys. 06 (2013) 064.

[5] R. Aaij *et al.* (LHCb Collaboration), Measurement of J/ψ production in pp collisions at $\sqrt{s} = 2.76$ TeV, J. High Energy Phys. 02 (2013) 041.

[6] R. Aaij *et al.* (LHCb Collaboration), Measurement of J/ψ production in pp collisions at $\sqrt{s} = 7$ TeV, Eur. Phys. J. C **71**, 1645 (2011).

[7] G. Aad *et al.* (ATLAS Collaboration), Measurement of the differential cross-sections of prompt and non-prompt production of J/ψ and $\psi(2S)$ in pp collisions at $\sqrt{s} = 7$ and 8 TeV with the ATLAS detector, Eur. Phys. J. C **76**, 283 (2016).

[8] V. Khachatryan *et al.* (CMS Collaboration), Measurement of J/ψ and $\psi(2S)$ Prompt Double-Differential Cross Sections in pp Collisions at $\sqrt{s} = 7$ TeV, Phys. Rev. Lett. **114**, 191802 (2015).

[9] B. Abelev *et al.* (ALICE Collaboration), Inclusive J/ψ production in pp collisions at $\sqrt{s} = 2.76$ TeV, Phys. Lett. B **718**, 295 (2012); CorrigendumPhys. Lett. B**748**, 472 (2015).

[10] G. T. Bodwin, E. Braaten, and G. P. Lepage, Rigorous QCD analysis of inclusive annihilation and production of heavy quarkonium, Phys. Rev. D **51**, 1125 (1995); Erratum, Phys. Rev. D **55**, 5853(E) (1997).

[11] P. Cho and A. K. Leibovich, Color octet quarkonia production, Phys. Rev. D **53**, 150 (1996).

[12] P. L. Cho and A. K. Leibovich, Color octet quarkonia production 2, Phys. Rev. D **53**, 6203 (1996).

[13] J. M. Campbell, F. Maltoni, and F. Tramontano, QCD Corrections to J/ψ and Υ Production at Hadron Colliders, Phys. Rev. Lett. **98**, 252002 (2007).

[14] J. P. Lansberg, On the mechanisms of heavy-quarkonium hadroproduction, Eur. Phys. J. C **61**, 693 (2009).
[15] B. Gong and J.-X. Wang, Next-to-Leading-Order QCD Corrections to J/ψ Polarization at Tevatron and Large Hadron Collider Energies, Phys. Rev. Lett. **100**, 232001 (2008).
[16] R. Aaij *et al.* (LHCb Collaboration), Measurement of J/ψ polarization in pp collisions at $\sqrt{s} = 7$ TeV, Eur. Phys. J. C **73**, 2631 (2013).
[17] B. Abelev *et al.* (ALICE Collaboration), J/ψ Polarization in pp Collisions at $\sqrt{s} = 7$ TeV, Phys. Rev. Lett. **108**, 082001 (2012).
[18] A. Abulencia *et al.* (CDF Collaboration), Polarization of J/ψ and $\psi(2S)$ Mesons Produced in $p\bar{p}$ Collisions at $\sqrt{s} = 1.96$ TeV, Phys. Rev. Lett. **99**, 132001 (2007).
[19] S. Chatrchyan *et al.* (CMS Collaboration), Measurement of the prompt J/ψ and $\psi(2S)$ polarizations in pp collisions at $\sqrt{s} = 7$ TeV, Phys. Lett. B **727**, 381 (2013).
[20] A. Andronic *et al.*, Heavy-flavour and quarkonium production in the LHC era: From proton-proton to heavy-ion collisions, Eur. Phys. J. C **76**, 107 (2016).
[21] R. Aaij *et al.* (LHCb Collaboration), Study of J/ψ production and cold nuclear matter effects in pPb collisions at $\sqrt{s_{\mathrm{NN}}} = 5$ TeV, J. High Energy Phys. 02 (2014) 072.
[22] R. Aaij *et al.* (LHCb Collaboration), Study of $\psi(2S)$ production cross-sections and cold nuclear matter effects in pPb collisions at $\sqrt{s_{\mathrm{NN}}} = 5$ TeV, J. High Energy Phys. 03 (2016) 133.
[23] G. Aad *et al.* (ATLAS Collaboration), Measurement of differential J/ψ production cross sections and forward-backward ratios in p-Pb collisions with the ATLAS detector, Phys. Rev. C **92**, 034904 (2015).
[24] G. Aad *et al.* (ATLAS Collaboration), Measurement of the centrality dependence of J/ψ yields and observation of Z production in lead-lead collisions with the ATLAS detector at the LHC, Phys. Lett. B **697**, 294 (2011).
[25] V. Khachatryan *et al.* (CMS Collaboration), Measurement of Prompt $\psi(2S) \to J/\psi$ Yield Ratios in Pb-Pb and $p-p$ Collisions at $\sqrt{s_{NN}} = 2.76$ TeV, Phys. Rev. Lett. **113**, 262301 (2014).
[26] A. M. Sirunyan *et al.* (CMS Collaboration), Relative modification of prompt $\psi(2S)$ and J/ψ yields from pp to PbPb collisions at $\sqrt{s_{\mathrm{NN}}} = 5.02$ TeV, arXiv:1611.01438.
[27] C. H. Kom, A. Kulesza, and W. J. Stirling, Prospects for observation of double parton scattering with four-muon final states at LHCb, Eur. Phys. J. C **71**, 1802 (2011).
[28] J.-P. Lansberg and H.-S. Shao, J/ψ-pair production at large momenta: Indications for double parton scatterings and large ^5_s contributions, Phys. Lett. B **751**, 479 (2015).
[29] R. Aaij *et al.* (LHCb Collaboration), Measurement of the J/ψ pair production cross-section in pp collisions at $\sqrt{s} = 13$ TeV, arXiv:1612.07451.
[30] V. M. Abazov *et al.* (D0 Collaboration), Observation and studies of double J/ψ production at the Tevatron, Phys. Rev. D **90**, 111101 (2014).
[31] V. Khachatryan *et al.* (CMS Collaboration), Measurement of prompt J/ψ pair production in pp collisions at $\sqrt{s} = 7$ TeV, J. High Energy Phys. 09 (2014) 094.
[32] R. Bain, L. Dai, A. Hornig, A. K. Leibovich, Y. Makris, and T. Mehen, Analytic and Monte Carlo studies of jets with heavy mesons and quarkonia, J. High Energy Phys. 06 (2016) 121.
[33] P. Ernström and L. Lönnblad, Generating heavy quarkonia in a perturbative QCD cascade, Z. Phys. C **75**, 51 (1997).
[34] M. Baumgart, A. K. Leibovich, T. Mehen, and I. Z. Rothstein, Probing quarkonium production mechanisms with jet substructure, J. High Energy Phys. 11 (2014) 003.
[35] M. Cacciari, G. P. Salam, and G. Soyez, The anti-k_T jet clustering algorithm, J. High Energy Phys. 04 (2008) 063.
[36] A. A. Alves Jr. *et al.* (LHCb Collaboration), The LHCb detector at the LHC, J. Instrum. **3**, S08005 (2008).
[37] R. Aaij *et al.* (LHCb Collaboration), LHCb detector performance, Int. J. Mod. Phys. A **30**, 1530022 (2015).
[38] T. Sjöstrand, S. Mrenna, and P. Skands, PYTHIA 6.4 physics and manual, J. High Energy Phys. 05 (2006) 026; T. Sjöstrand, S. Mrenna, and P. Skands, A brief introduction to PYTHIA 8.1, Comput. Phys. Commun. **178**, 852 (2008).
[39] I. Belyaev *et al.*, Handling of the generation of primary events in Gauss, the LHCb simulation framework, J. Phys. Conf. Ser. **331**, 032047 (2011).
[40] D. J. Lange, The EvtGen particle decay simulation package, Nucl. Instrum. Methods Phys. Res., Sect. A **462**, 152 (2001).
[41] P. Golonka and Z. Was, PHOTOS Monte Carlo: A precision tool for QED corrections in Z and W decays, Eur. Phys. J. C **45**, 97 (2006).
[42] J. Allison *et al.* (Geant4 Collaboration), Geant4 developments and applications, IEEE Trans. Nucl. Sci. **53**, 270 (2006); S. Agostinelli *et al.* (Geant4 Collaboration), Geant4: A simulation toolkit, Nucl. Instrum. Methods Phys. Res., Sect. A **506**, 250 (2003).
[43] M. Clemencic, G. Corti, S. Easo, C. R. Jones, S. Miglioranzi, M. Pappagallo, and P. Robbe, The LHCb simulation application, Gauss: Design, evolution and experience, J. Phys. Conf. Ser. **331**, 032023 (2011).
[44] R. Aaij *et al.*, The LHCb trigger and its performance in 2011, J. Instrum. **8**, P04022 (2013).
[45] C. Patrignani *et al.* (Particle Data Group), Review of particle physics, Chin. Phys. C **40**, 100001 (2016).
[46] G. Dujany and B. Storaci, Real-time alignment and calibration of the LHCb Detector in Run II, J. Phys. Conf. Ser. **664**, 082010 (2015).
[47] R. Aaij *et al.*, Tesla: An application for real-time data analysis in high energy physics, Comput. Phys. Commun. **208**, 35 (2016).
[48] R. Aaij *et al.* (LHCb Collaboration), Study of forward $Z+$jet production in pp collisions at $\sqrt{s} = 7$ TeV, J. High Energy Phys. 01 (2014) 033.
[49] M. Cacciari, G. P. Salam, and G. Soyez, FastJet user manual, Eur. Phys. J. C **72**, 1896 (2012).
[50] G. D'Agostini, A multidimensional unfolding method based on Bayes' theorem, Nucl. Instrum. Methods Phys. Res., Sect. A **362**, 487 (1995).
[51] T. Adye, Unfolding algorithms and tests using RooUnfold, arXiv:1105.1160.
[52] See Supplemental Material at http://link.aps.org/supplemental/10.1103/PhysRevLett.118.192001 for details on unfolding the detector response, the uncertainties on the

PYTHIA predictions, and for additional plots and numerical results.

[53] T. Skwarnicki, Ph.D. thesis, Institute of Nuclear Physics, Krakow, 1986, DESY-F31-86-02.

[54] R. Aaij *et al.* (LHCb Collaboration), Measurement of the track reconstruction efficiency at LHCb, J. Instrum. **10**, P02007 (2015).

[55] P. Nason *et al.*, Bottom production, arXiv:hep-ph/0003142.

[56] V. Khachatryan *et al.* (CMS Collaboration), Measurement of the top quark mass using charged particles in pp collisions at $\sqrt{s} = 8$ TeV, Phys. Rev. D **93**, 092006 (2016).

[57] R. Aaij *et al.* (LHCb Collaboration), Measurement of the forward energy flow in pp collisions at $\sqrt{s} = 7$ TeV, Eur. Phys. J. C **73**, 2421 (2013).

[58] H.-S. Shao, HELAC-Onia 2.0: An upgraded matrix-element and event generator for heavy quarkonium physics, Comput. Phys. Commun. **198**, 238 (2016).

[59] R. Bain *et al.*, NRQCD confronts LHCb data on quarkonium production within jets, arXiv:1702.05525.

[60] Z.-B. Kang *et al.*, J/ψ production and polarization within a jet, arXiv:1702.03287.

[61] P. Ilten, N. L. Rodd, J. Thaler, and M. Williams, Disentangling heavy flavor at colliders, arXiv:1702.02947.

R. Aaij,[40] B. Adeva,[39] M. Adinolfi,[48] Z. Ajaltouni,[5] S. Akar,[59] J. Albrecht,[10] F. Alessio,[40] M. Alexander,[53] S. Ali,[43] G. Alkhazov,[31] P. Alvarez Cartelle,[55] A. A. Alves Jr.,[59] S. Amato,[2] S. Amerio,[23] Y. Amhis,[7] L. An,[3] L. Anderlini,[18] G. Andreassi,[41] M. Andreotti,[17,a] J. E. Andrews,[60] R. B. Appleby,[56] F. Archilli,[43] P. d'Argent,[12] J. Arnau Romeu,[6] A. Artamonov,[37] M. Artuso,[61] E. Aslanides,[6] G. Auriemma,[26] M. Baalouch,[5] I. Babuschkin,[56] S. Bachmann,[12] J. J. Back,[50] A. Badalov,[38] C. Baesso,[62] S. Baker,[55] V. Balagura,[7,b] W. Baldini,[17] A. Baranov,[35] R. J. Barlow,[56] C. Barschel,[40] S. Barsuk,[7] W. Barter,[56] F. Baryshnikov,[32] M. Baszczyk,[27] V. Batozskaya,[29] B. Batsukh,[61] V. Battista,[41] A. Bay,[41] L. Beaucourt,[4] J. Beddow,[53] F. Bedeschi,[24] I. Bediaga,[1] A. Beiter,[61] L. J. Bel,[43] V. Bellee,[41] N. Belloli,[21,c] K. Belous,[37] I. Belyaev,[32] E. Ben-Haim,[8] G. Bencivenni,[19] S. Benson,[43] S. Beranek,[9] A. Berezhnoy,[33] R. Bernet,[42] A. Bertolin,[23] C. Betancourt,[42] F. Betti,[15] M.-O. Bettler,[40] M. van Beuzekom,[43] Ia. Bezshyiko,[42] S. Bifani,[47] P. Billoir,[8] T. Bird,[56] A. Birnkraut,[10] A. Bitadze,[56] A. Bizzeti,[18,d] T. Blake,[50] F. Blanc,[41] J. Blouw,[11] S. Blusk,[61] V. Bocci,[26] T. Boettcher,[58] A. Bondar,[36,e] N. Bondar,[31,40] W. Bonivento,[16] I. Bordyuzhin,[32] A. Borgheresi,[21,c] S. Borghi,[56] M. Borisyak,[35] M. Borsato,[39] F. Bossu,[7] M. Boubdir,[9] T. J. V. Bowcock,[54] E. Bowen,[42] C. Bozzi,[17,40] S. Braun,[12] M. Britsch,[12] T. Britton,[61] J. Brodzicka,[56] E. Buchanan,[48] C. Burr,[56] A. Bursche,[2] J. Buytaert,[40] S. Cadeddu,[16] R. Calabrese,[17,a] M. Calvi,[21,c] M. Calvo Gomez,[38,f] A. Camboni,[38] P. Campana,[19] D. H. Campora Perez,[40] L. Capriotti,[56] A. Carbone,[15,g] G. Carboni,[25,h] R. Cardinale,[20,i] A. Cardini,[16] P. Carniti,[21,c] L. Carson,[52] K. Carvalho Akiba,[2] G. Casse,[54] L. Cassina,[21,c] L. Castillo Garcia,[41] M. Cattaneo,[40] G. Cavallero,[20] R. Cenci,[24,j] D. Chamont,[7] M. Charles,[8] Ph. Charpentier,[40] G. Chatzikonstantinidis,[47] M. Chefdeville,[4] S. Chen,[56] S.-F. Cheung,[57] V. Chobanova,[39] M. Chrzaszcz,[42,27] X. Cid Vidal,[39] G. Ciezarek,[43] P. E. L. Clarke,[52] M. Clemencic,[40] H. V. Cliff,[49] J. Closier,[40] V. Coco,[59] J. Cogan,[6] E. Cogneras,[5] V. Cogoni,[16,40,k] L. Cojocariu,[30] G. Collazuol,[23,l] P. Collins,[40] A. Comerma-Montells,[12] A. Contu,[40] A. Cook,[48] G. Coombs,[40] S. Coquereau,[38] G. Corti,[40] M. Corvo,[17,a] C. M. Costa Sobral,[50] B. Couturier,[40] G. A. Cowan,[52] D. C. Craik,[52] A. Crocombe,[50] M. Cruz Torres,[62] S. Cunliffe,[55] R. Currie,[55] C. D'Ambrosio,[40] F. Da Cunha Marinho,[2] E. Dall'Occo,[43] J. Dalseno,[48] P. N. Y. David,[43] A. Davis,[3] K. De Bruyn,[6] S. De Capua,[56] M. De Cian,[12] J. M. De Miranda,[1] L. De Paula,[2] M. De Serio,[14,m] P. De Simone,[19] C. T. Dean,[53] D. Decamp,[4] M. Deckenhoff,[10] L. Del Buono,[8] M. Demmer,[10] A. Dendek,[28] D. Derkach,[35] O. Deschamps,[5] F. Dettori,[40] B. Dey,[22] A. Di Canto,[40] H. Dijkstra,[40] F. Dordei,[40] M. Dorigo,[41] A. Dosil Suárez,[39] A. Dovbnya,[45] K. Dreimanis,[54] L. Dufour,[43] G. Dujany,[56] K. Dungs,[40] P. Durante,[40] R. Dzhelyadin,[37] A. Dziurda,[40] A. Dzyuba,[31] N. Déléage,[4] S. Easo,[51] M. Ebert,[52] U. Egede,[55] V. Egorychev,[32] S. Eidelman,[36,e] S. Eisenhardt,[52] U. Eitschberger,[10] R. Ekelhof,[10] L. Eklund,[53] S. Ely,[61] S. Esen,[12] H. M. Evans,[49] T. Evans,[57] A. Falabella,[15] N. Farley,[47] S. Farry,[54] R. Fay,[54] D. Fazzini,[21,c] D. Ferguson,[52] G. Fernandez,[38] A. Fernandez Prieto,[39] F. Ferrari,[15,40] F. Ferreira Rodrigues,[2] M. Ferro-Luzzi,[40] S. Filippov,[34] R. A. Fini,[14] M. Fiore,[17,a] M. Fiorini,[17,a] M. Firlej,[28] C. Fitzpatrick,[41] T. Fiutowski,[28] F. Fleuret,[7,n] K. Fohl,[40] M. Fontana,[16,40] F. Fontanelli,[20,i] D. C. Forshaw,[61] R. Forty,[40] V. Franco Lima,[54] M. Frank,[40] C. Frei,[40] J. Fu,[22,o] W. Funk,[40] E. Furfaro,[25,h] C. Färber,[40] A. Gallas Torreira,[39] D. Galli,[15,g] S. Gallorini,[23] S. Gambetta,[52] M. Gandelman,[2] P. Gandini,[57] Y. Gao,[3] L. M. Garcia Martin,[69] J. García Pardiñas,[39] J. Garra Tico,[49] L. Garrido,[38] P. J. Garsed,[49] D. Gascon,[38] C. Gaspar,[40] L. Gavardi,[10] G. Gazzoni,[5] D. Gerick,[12] E. Gersabeck,[12] M. Gersabeck,[56] T. Gershon,[50] Ph. Ghez,[4] S. Gianì,[41] V. Gibson,[49] O. G. Girard,[41] L. Giubega,[30] K. Gizdov,[52] V. V. Gligorov,[8] D. Golubkov,[32] A. Golutvin,[55,40] A. Gomes,[1,p] I. V. Gorelov,[33] C. Gotti,[21,c] E. Govorkova,[43] R. Graciani Diaz,[38] L. A. Granado Cardoso,[40] E. Graugés,[38] E. Graverini,[42] G. Graziani,[18] A. Grecu,[30] R. Greim,[9] P. Griffith,[47] L. Grillo,[21,40,c] B. R. Gruberg Cazon,[57]

O. Grünberg,[67] E. Gushchin,[34] Yu. Guz,[37] T. Gys,[40] C. Göbel,[62] T. Hadavizadeh,[57] C. Hadjivasiliou,[5] G. Haefeli,[41] C. Haen,[40] S. C. Haines,[49] B. Hamilton,[60] X. Han,[12] S. Hansmann-Menzemer,[12] N. Harnew,[57] S. T. Harnew,[48] J. Harrison,[56] M. Hatch,[40] J. He,[63] T. Head,[41] A. Heister,[9] K. Hennessy,[54] P. Henrard,[5] L. Henry,[8] E. van Herwijnen,[40] M. Heß,[67] A. Hicheur,[2] D. Hill,[57] C. Hombach,[56] H. Hopchev,[41] W. Hulsbergen,[43] T. Humair,[55] M. Hushchyn,[35] D. Hutchcroft,[54] M. Idzik,[28] P. Ilten,[58] R. Jacobsson,[40] A. Jaeger,[12] J. Jalocha,[57] E. Jans,[43] A. Jawahery,[60] F. Jiang,[3] M. John,[57] D. Johnson,[40] C. R. Jones,[49] C. Joram,[40] B. Jost,[40] N. Jurik,[57] S. Kandybei,[45] M. Karacson,[40] J. M. Kariuki,[48] S. Karodia,[53] M. Kecke,[12] M. Kelsey,[61] M. Kenzie,[49] T. Ketel,[44] E. Khairullin,[35] B. Khanji,[12] C. Khurewathanakul,[41] T. Kirn,[9] S. Klaver,[56] K. Klimaszewski,[29] T. Klimkovich,[11] S. Koliiev,[46] M. Kolpin,[12] I. Komarov,[41] P. Koppenburg,[43] A. Kosmyntseva,[32] A. Kozachuk,[33] M. Kozeiha,[5] L. Kravchuk,[34] K. Kreplin,[12] M. Kreps,[50] P. Krokovny,[36,e] F. Kruse,[10] W. Krzemien,[29] W. Kucewicz,[27,q] M. Kucharczyk,[27] V. Kudryavtsev,[36,e] A. K. Kuonen,[41] K. Kurek,[29] T. Kvaratskheliya,[32,40] D. Lacarrere,[40] G. Lafferty,[56] A. Lai,[16] G. Lanfranchi,[19] C. Langenbruch,[9] T. Latham,[50] C. Lazzeroni,[47] R. Le Gac,[6] J. van Leerdam,[43] A. Leflat,[33,40] J. Lefrançois,[7] R. Lefèvre,[5] F. Lemaitre,[40] E. Lemos Cid,[39] O. Leroy,[6] T. Lesiak,[27] B. Leverington,[12] T. Li,[3] Y. Li,[7] T. Likhomanenko,[35,68] R. Lindner,[40] C. Linn,[40] F. Lionetto,[42] X. Liu,[3] D. Loh,[50] I. Longstaff,[53] J. H. Lopes,[2] D. Lucchesi,[23,l] M. Lucio Martinez,[39] H. Luo,[52] A. Lupato,[23] E. Luppi,[17,a] O. Lupton,[40] A. Lusiani,[24] X. Lyu,[63] F. Machefert,[7] F. Maciuc,[30] O. Maev,[31] K. Maguire,[56] S. Malde,[57] A. Malinin,[68] T. Maltsev,[36] G. Manca,[16,k] G. Mancinelli,[6] P. Manning,[61] J. Maratas,[5,r] J. F. Marchand,[4] U. Marconi,[15] C. Marin Benito,[38] M. Marinangeli,[41] P. Marino,[24,j] J. Marks,[12] G. Martellotti,[26] M. Martin,[6] M. Martinelli,[41] D. Martinez Santos,[39] F. Martinez Vidal,[69] D. Martins Tostes,[2] L. M. Massacrier,[7] A. Massafferri,[1] R. Matev,[40] A. Mathad,[50] Z. Mathe,[40] C. Matteuzzi,[21] A. Mauri,[42] E. Maurice,[7,n] B. Maurin,[41] A. Mazurov,[47] M. McCann,[55,40] A. McNab,[56] R. McNulty,[13] B. Meadows,[59] F. Meier,[10] M. Meissner,[12] D. Melnychuk,[29] M. Merk,[43] A. Merli,[22,o] E. Michielin,[23] D. A. Milanes,[66] M.-N. Minard,[4] D. S. Mitzel,[12] A. Mogini,[8] J. Molina Rodriguez,[1] I. A. Monroy,[66] S. Monteil,[5] M. Morandin,[23] P. Morawski,[28] A. Mordà,[6] M. J. Morello,[24,j] O. Morgunova,[68] J. Moron,[28] A. B. Morris,[52] R. Mountain,[61] F. Muheim,[52] M. Mulder,[43] M. Mussini,[15] D. Müller,[56] J. Müller,[10] K. Müller,[42] V. Müller,[10] P. Naik,[48] T. Nakada,[41] R. Nandakumar,[51] A. Nandi,[57] I. Nasteva,[2] M. Needham,[52] N. Neri,[22] S. Neubert,[12] N. Neufeld,[40] M. Neuner,[12] T. D. Nguyen,[41] C. Nguyen-Mau,[41,s] S. Nieswand,[9] R. Niet,[10] N. Nikitin,[33] T. Nikodem,[12] A. Nogay,[68] A. Novoselov,[37] D. P. O'Hanlon,[50] A. Oblakowska-Mucha,[28] V. Obraztsov,[37] S. Ogilvy,[19] O. Okhrimenko,[46] R. Oldeman,[16,k] C. J. G. Onderwater,[70] J. M. Otalora Goicochea,[2] A. Otto,[40] P. Owen,[42] A. Oyanguren,[69] P. R. Pais,[41] A. Palano,[14,m] M. Palutan,[19] A. Papanestis,[51] M. Pappagallo,[14,m] L. L. Pappalardo,[17,a] W. Parker,[60] C. Parkes,[56] G. Passaleva,[18] A. Pastore,[14,m] G. D. Patel,[54] M. Patel,[55] C. Patrignani,[15,g] A. Pearce,[40] A. Pellegrino,[43] G. Penso,[26] M. Pepe Altarelli,[40] S. Perazzini,[40] P. Perret,[5] L. Pescatore,[47] K. Petridis,[48] A. Petrolini,[20,i] A. Petrov,[68] M. Petruzzo,[22,o] E. Picatoste Olloqui,[38] B. Pietrzyk,[4] M. Pikies,[27] D. Pinci,[26] A. Pistone,[20] A. Piucci,[12] V. Placinta,[30] S. Playfer,[52] M. Plo Casasus,[39] T. Poikela,[40] F. Polci,[8] A. Poluektov,[50,36] I. Polyakov,[61] E. Polycarpo,[2] G. J. Pomery,[48] S. Ponce,[40] A. Popov,[37] D. Popov,[11,40] B. Popovici,[30] S. Poslavskii,[37] C. Potterat,[2] E. Price,[48] J. D. Price,[54] J. Prisciandaro,[39] A. Pritchard,[54] C. Prouve,[48] V. Pugatch,[46] A. Puig Navarro,[42] G. Punzi,[24,t] W. Qian,[50] R. Quagliani,[7,48] B. Rachwal,[27] J. H. Rademacker,[48] M. Rama,[24] M. Ramos Pernas,[39] M. S. Rangel,[2] I. Raniuk,[45] F. Ratnikov,[35] G. Raven,[44] F. Redi,[55] S. Reichert,[10] A. C. dos Reis,[1] C. Remon Alepuz,[69] V. Renaudin,[7] S. Ricciardi,[51] S. Richards,[48] M. Rihl,[40] K. Rinnert,[54] V. Rives Molina,[38] P. Robbe,[7,40] A. B. Rodrigues,[1] E. Rodrigues,[59] J. A. Rodriguez Lopez,[66] P. Rodriguez Perez,[56] A. Rogozhnikov,[35] S. Roiser,[40] A. Rollings,[57] V. Romanovskiy,[37] A. Romero Vidal,[39] J. W. Ronayne,[13] M. Rotondo,[19] M. S. Rudolph,[61] T. Ruf,[40] P. Ruiz Valls,[69] J. J. Saborido Silva,[39] E. Sadykhov,[32] N. Sagidova,[31] B. Saitta,[16,k] V. Salustino Guimaraes,[1] D. Sanchez Gonzalo,[38] C. Sanchez Mayordomo,[69] B. Sanmartin Sedes,[39] R. Santacesaria,[26] C. Santamarina Rios,[39] M. Santimaria,[19] E. Santovetti,[25,h] A. Sarti,[19,u] C. Satriano,[26,v] A. Satta,[25] D. M. Saunders,[48] D. Savrina,[32,33] S. Schael,[9] M. Schellenberg,[10] M. Schiller,[53] H. Schindler,[40] M. Schlupp,[10] M. Schmelling,[11] T. Schmelzer,[10] B. Schmidt,[40] O. Schneider,[41] A. Schopper,[40] H. F. Schreiner,[59] K. Schubert,[10] M. Schubiger,[41] M.-H. Schune,[7] R. Schwemmer,[40] B. Sciascia,[19] A. Sciubba,[26,u] A. Semennikov,[32] A. Sergi,[47] N. Serra,[42] J. Serrano,[6] L. Sestini,[23] P. Seyfert,[21] M. Shapkin,[37] I. Shapoval,[45] Y. Shcheglov,[31] T. Shears,[54] L. Shekhtman,[36,e] V. Shevchenko,[68] B. G. Siddi,[17,40] R. Silva Coutinho,[42] L. Silva de Oliveira,[2] G. Simi,[23,l] S. Simone,[14,m] M. Sirendi,[49] N. Skidmore,[48] T. Skwarnicki,[61] E. Smith,[55] I. T. Smith,[52] J. Smith,[49] M. Smith,[55] l. Soares Lavra,[1] M. D. Sokoloff,[59] F. J. P. Soler,[53] B. Souza De Paula,[2] B. Spaan,[10] P. Spradlin,[53] S. Sridharan,[40] F. Stagni,[40] M. Stahl,[12] S. Stahl,[40] P. Stefko,[41] S. Stefkova,[55] O. Steinkamp,[42] S. Stemmle,[12] O. Stenyakin,[37] H. Stevens,[10] S. Stevenson,[57] S. Stoica,[30] S. Stone,[61] B. Storaci,[42] S. Stracka,[24,t] M. E. Stramaglia,[41] M. Straticiuc,[30] U. Straumann,[42] L. Sun,[64]

W. Sutcliffe,[55] K. Swientek,[28] V. Syropoulos,[44] M. Szczekowski,[29] T. Szumlak,[28] S. T'Jampens,[4] A. Tayduganov,[6] T. Tekampe,[10] G. Tellarini,[17,a] F. Teubert,[40] E. Thomas,[40] J. van Tilburg,[43] M. J. Tilley,[55] V. Tisserand,[4] M. Tobin,[41] S. Tolk,[49] L. Tomassetti,[17,a] D. Tonelli,[40] S. Topp-Joergensen,[57] F. Toriello,[61] E. Tournefier,[4] S. Tourneur,[41] K. Trabelsi,[41] M. Traill,[53] M. T. Tran,[41] M. Tresch,[42] A. Trisovic,[40] A. Tsaregorodtsev,[6] P. Tsopelas,[43] A. Tully,[49] N. Tuning,[43] A. Ukleja,[29] A. Ustyuzhanin,[35] U. Uwer,[12] C. Vacca,[16,k] V. Vagnoni,[15,40] A. Valassi,[40] S. Valat,[40] G. Valenti,[15] R. Vazquez Gomez,[19] P. Vazquez Regueiro,[39] S. Vecchi,[17] M. van Veghel,[43] J. J. Velthuis,[48] M. Veltri,[18,w] G. Veneziano,[57] A. Venkateswaran,[61] M. Vernet,[5] M. Vesterinen,[12] J. V. Viana Barbosa,[40] B. Viaud,[7] D. Vieira,[63] M. Vieites Diaz,[39] H. Viemann,[67] X. Vilasis-Cardona,[38,f] M. Vitti,[49] V. Volkov,[33] A. Vollhardt,[42] B. Voneki,[40] A. Vorobyev,[31] V. Vorobyev,[36,e] C. Voß,[9] J. A. de Vries,[43] C. Vázquez Sierra,[39] R. Waldi,[67] C. Wallace,[50] R. Wallace,[13] J. Walsh,[24] J. Wang,[61] D. R. Ward,[49] H. M. Wark,[54] N. K. Watson,[47] D. Websdale,[55] A. Weiden,[42] M. Whitehead,[40] J. Wicht,[50] G. Wilkinson,[57,40] M. Wilkinson,[61] M. Williams,[40] M. P. Williams,[47] M. Williams,[58] T. Williams,[47] F. F. Wilson,[51] J. Wimberley,[60] J. Wishahi,[10] W. Wislicki,[29] M. Witek,[27] G. Wormser,[7] S. A. Wotton,[49] K. Wraight,[53] K. Wyllie,[40] Y. Xie,[65] Z. Xing,[61] Z. Xu,[4] Z. Yang,[3] Y. Yao,[61] H. Yin,[65] J. Yu,[65] X. Yuan,[36,e] O. Yushchenko,[37] K. A. Zarebski,[47] M. Zavertyaev,[11,b] L. Zhang,[3] Y. Zhang,[7] Y. Zhang,[63] A. Zhelezov,[12] Y. Zheng,[63] X. Zhu,[3] V. Zhukov,[33] and S. Zucchelli[15]

(LHCb Collaboration)

[1]*Centro Brasileiro de Pesquisas Físicas (CBPF), Rio de Janeiro, Brazil*
[2]*Universidade Federal do Rio de Janeiro (UFRJ), Rio de Janeiro, Brazil*
[3]*Center for High Energy Physics, Tsinghua University, Beijing, China*
[4]*LAPP, Université Savoie Mont-Blanc, CNRS/IN2P3, Annecy-Le-Vieux, France*
[5]*Clermont Université, Université Blaise Pascal, CNRS/IN2P3, LPC, Clermont-Ferrand, France*
[6]*CPPM, Aix-Marseille Université, CNRS/IN2P3, Marseille, France*
[7]*LAL, Université Paris-Sud, CNRS/IN2P3, Orsay, France*
[8]*LPNHE, Université Pierre et Marie Curie, Université Paris Diderot, CNRS/IN2P3, Paris, France*
[9]*I. Physikalisches Institut, RWTH Aachen University, Aachen, Germany*
[10]*Fakultät Physik, Technische Universität Dortmund, Dortmund, Germany*
[11]*Max-Planck-Institut für Kernphysik (MPIK), Heidelberg, Germany*
[12]*Physikalisches Institut, Ruprecht-Karls-Universität Heidelberg, Heidelberg, Germany*
[13]*School of Physics, University College Dublin, Dublin, Ireland*
[14]*Sezione INFN di Bari, Bari, Italy*
[15]*Sezione INFN di Bologna, Bologna, Italy*
[16]*Sezione INFN di Cagliari, Cagliari, Italy*
[17]*Sezione INFN di Ferrara, Ferrara, Italy*
[18]*Sezione INFN di Firenze, Firenze, Italy*
[19]*Laboratori Nazionali dell'INFN di Frascati, Frascati, Italy*
[20]*Sezione INFN di Genova, Genova, Italy*
[21]*Sezione INFN di Milano Bicocca, Milano, Italy*
[22]*Sezione INFN di Milano, Milano, Italy*
[23]*Sezione INFN di Padova, Padova, Italy*
[24]*Sezione INFN di Pisa, Pisa, Italy*
[25]*Sezione INFN di Roma Tor Vergata, Roma, Italy*
[26]*Sezione INFN di Roma La Sapienza, Roma, Italy*
[27]*Henryk Niewodniczanski Institute of Nuclear Physics Polish Academy of Sciences, Kraków, Poland*
[28]*AGH - University of Science and Technology, Faculty of Physics and Applied Computer Science, Kraków, Poland*
[29]*National Center for Nuclear Research (NCBJ), Warsaw, Poland*
[30]*Horia Hulubei National Institute of Physics and Nuclear Engineering, Bucharest-Magurele, Romania*
[31]*Petersburg Nuclear Physics Institute (PNPI), Gatchina, Russia*
[32]*Institute of Theoretical and Experimental Physics (ITEP), Moscow, Russia*
[33]*Institute of Nuclear Physics, Moscow State University (SINP MSU), Moscow, Russia*
[34]*Institute for Nuclear Research of the Russian Academy of Sciences (INR RAN), Moscow, Russia*
[35]*Yandex School of Data Analysis, Moscow, Russia*
[36]*Budker Institute of Nuclear Physics (SB RAS), Novosibirsk, Russia*
[37]*Institute for High Energy Physics (IHEP), Protvino, Russia*
[38]*ICCUB, Universitat de Barcelona, Barcelona, Spain*

[39]Universidad de Santiago de Compostela, Santiago de Compostela, Spain
[40]European Organization for Nuclear Research (CERN), Geneva, Switzerland
[41]Institute of Physics, Ecole Polytechnique Fédérale de Lausanne (EPFL), Lausanne, Switzerland
[42]Physik-Institut, Universität Zürich, Zürich, Switzerland
[43]Nikhef National Institute for Subatomic Physics, Amsterdam, Netherlands
[44]Nikhef National Institute for Subatomic Physics and VU University Amsterdam, Amsterdam, Netherlands
[45]NSC Kharkiv Institute of Physics and Technology (NSC KIPT), Kharkiv, Ukraine
[46]Institute for Nuclear Research of the National Academy of Sciences (KINR), Kyiv, Ukraine
[47]University of Birmingham, Birmingham, United Kingdom
[48]H.H. Wills Physics Laboratory, University of Bristol, Bristol, United Kingdom
[49]Cavendish Laboratory, University of Cambridge, Cambridge, United Kingdom
[50]Department of Physics, University of Warwick, Coventry, United Kingdom
[51]STFC Rutherford Appleton Laboratory, Didcot, United Kingdom
[52]School of Physics and Astronomy, University of Edinburgh, Edinburgh, United Kingdom
[53]School of Physics and Astronomy, University of Glasgow, Glasgow, United Kingdom
[54]Oliver Lodge Laboratory, University of Liverpool, Liverpool, United Kingdom
[55]Imperial College London, London, United Kingdom
[56]School of Physics and Astronomy, University of Manchester, Manchester, United Kingdom
[57]Department of Physics, University of Oxford, Oxford, United Kingdom
[58]Massachusetts Institute of Technology, Cambridge, Massachusetts, USA
[59]University of Cincinnati, Cincinnati, Ohio, USA
[60]University of Maryland, College Park, Maryland, USA
[61]Syracuse University, Syracuse, New York, USA
[62]Pontifícia Universidade Católica do Rio de Janeiro (PUC-Rio), Rio de Janeiro, Brazil (associated with Institution Universidade Federal do Rio de Janeiro (UFRJ), Rio de Janeiro, Brazil)
[63]University of Chinese Academy of Sciences, Beijing, China (associated with Institution Center for High Energy Physics, Tsinghua University, Beijing, China)
[64]School of Physics and Technology, Wuhan University, Wuhan, China (associated with Institution Center for High Energy Physics, Tsinghua University, Beijing, China)
[65]Institute of Particle Physics, Central China Normal University, Wuhan, Hubei, China (associated with Institution Center for High Energy Physics, Tsinghua University, Beijing, China)
[66]Departamento de Fisica, Universidad Nacional de Colombia, Bogota, Colombia (associated with Institution LPNHE, Université Pierre et Marie Curie, Université Paris Diderot, CNRS/IN2P3, Paris, France)
[67]Institut für Physik, Universität Rostock, Rostock, Germany (associated with Institution Physikalisches Institut, Ruprecht-Karls-Universität Heidelberg, Heidelberg, Germany)
[68]National Research Centre Kurchatov Institute, Moscow, Russia [associated with Institution Institute of Theoretical and Experimental Physics (ITEP), Moscow, Russia]
[69]Instituto de Fisica Corpuscular, Centro Mixto Universidad de Valencia - CSIC, Valencia, Spain (associated with Institution ICCUB, Universitat de Barcelona, Barcelona, Spain)
[70]Van Swinderen Institute, University of Groningen, Groningen, Netherlands (associated with Institution Nikhef National Institute for Subatomic Physics, Amsterdam, Netherlands)

[a]Also at Università di Ferrara, Ferrara, Italy.
[b]Also at P.N. Lebedev Physical Institute, Russian Academy of Science (LPI RAS), Moscow, Russia.
[c]Also at Università di Milano Bicocca, Milano, Italy.
[d]Also at Università di Modena e Reggio Emilia, Modena, Italy.
[e]Also at Novosibirsk State University, Novosibirsk, Russia.
[f]Also at LIFAELS, La Salle, Universitat Ramon Llull, Barcelona, Spain.
[g]Also at Università di Bologna, Bologna, Italy.
[h]Also at Università di Roma Tor Vergata, Roma, Italy.
[i]Also at Università di Genova, Genova, Italy.
[j]Also at Scuola Normale Superiore, Pisa, Italy.
[k]Also at Università di Cagliari, Cagliari, Italy.
[l]Also at Università di Padova, Padova, Italy.
[m]Also at Università di Bari, Bari, Italy.
[n]Also at Laboratoire Leprince-Ringuet, Palaiseau, France.

[o]Also at Università degli Studi di Milano, Milano, Italy.
[p]Also at Universidade Federal do Triângulo Mineiro (UFTM), Uberaba-MG, Brazil.
[q]Also at AGH—University of Science and Technology, Faculty of Computer Science, Electronics and Telecommunications, Kraków, Poland.
[r]Also at Iligan Institute of Technology (IIT), Iligan, Philippines.
[s]Also at Hanoi University of Science, Hanoi, Viet Nam.
[t]Also at Università di Pisa, Pisa, Italy.
[u]Also at Università di Roma La Sapienza, Roma, Italy.
[v]Also at Università della Basilicata, Potenza, Italy.
[w]Also at Università di Urbino, Urbino, Italy.